Journal of Zhejiang University-SCIENCE A (Applied Physics & Engineering)
ISSN 1673-565X (Print); ISSN 1862-1775 (Online)
www.jzus.zju.edu.cn; link.springer.com
E-mail: jzus_a@zju.edu.cn

Application of an interpretable artificial neural network to predict the interface strength of a near-surface mounted fiber-reinforced polymer to concrete joint*#

Miao SU[1,2], Hui PENG[1], Shao-fan LI†‡[2]

[1]School of Civil Engineering, Changsha University of Science and Technology, Changsha 410114, China

[2]Department of Civil and Environmental Engineering, University of California, Berkeley, CA 94720, USA

†E-mail: shaofan@berkeley.edu

Received June 1, 2020; Revision accepted Aug. 26, 2020; Crosschecked May 20, 2021

Abstract: Accurately estimating the interfacial bond capacity of the near-surface mounted (NSM) carbon fiber-reinforced polymer (CFRP) to concrete joint is a fundamental task in the strengthening and retrofit of existing reinforced concrete (RC) structures. The machine learning (ML) approach may provide an alternative to the commonly used semi-empirical or semi-analytical methods. Therefore, in this work we have developed a predictive model based on an artificial neural network (ANN) approach, i.e. using a back propagation neural network (BPNN), to map the complex data pattern obtained from an NSM CFRP to concrete joint. It involves a set of nine material and geometric input parameters and one output value. Moreover, by employing the neural interpretation diagram (NID) technique, the BPNN model becomes interpretable, as the influence of each input variable on the model can be tracked and quantified based on the connection weights of the neural network. An extensive database including 163 pull-out testing samples, collected from the authors' research group and from published results in the literature, is used to train and verify the ANN. Our results show that the prediction given by the BPNN model agrees well with the experimental data and yields a coefficient of determination of 0.957 on the whole database. After removing one non-significant feature, the BPNN becomes even more computationally efficient and accurate. In addition, compared with the existed semi-analytical model, the ANN-based approach demonstrates a more accurate estimation. Therefore, the proposed ML method may be a promising alternative for predicting the bond strength of NSM CFRP to concrete joint for structural engineers.

Key words: Fiber-reinforced polymer (FRP); Bond strength; Machine learning (ML); Neural interpretation diagram (NID); Regression; Feature importance; Connection weights approach

https://doi.org/10.1631/jzus.A2000245 **CLC number:** TU599

1 Introduction

Many techniques for strengthening existing reinforced concrete (RC) structures with various fiber-reinforced polymer (FRP) composites have been developed in recent years (Ghasemi et al., 2014; Al-Mahaidi and Kalfat 2018; Zhang et al., 2018), and externally bonding (EB) an FRP fabric or plate onto the surface of the structure is the most commonly used technique (Wu et al., 2010; Bilotta et al., 2011). In particular, the carbon fiber-reinforced polymer (CFRP) strip, is the most popular of various FRP

‡ Corresponding author

*Project supported by the National Natural Science Foundation of China (No. 51808056), the Hunan Provincial Natural Science Foundation of China (No. 2020JJ5583), the Research Foundation of Education Bureau of Hunan Province (No. 19B012), and the China Scholarship Council (No. 201808430232)

Electronic supplementary materials: The online version of this article (https://doi.org/10.1631/jzus.A2000245) contains supplementary materials, which are available to authorized users

ORCID: Miao SU, https://orcid.org/0000-0002-8750-7204; Shao-fan LI, https://orcid.org/0000-0002-6950-1474

materials due to its high tensile strength and stiffness (Chen et al., 2019). However, the cohesive debonding of the FRP from the adjacent concrete leading to premature failure of the EB strengthening technology has become a crucial and persistent problem in practical engineering. Against that background, the near-surface mounted (NSM) FRP strengthening technique, regarded as a promising alternative to the EB FRP strengthening method, has developed quickly over the past ten years (Ali et al., 2008; Zhang et al., 2017). In the NSM strengthening technique, as shown in Fig. 1, the FRP laminates are embedded into grooves that are first cut in the concrete cover of RC structures. The gap between the FRP laminate and the groove is filled with adhesive, for example, epoxy paste or cement grout (de Lorenzis and Teng, 2007). Compared with the EB technology, the RC structures strengthened by this NSM method usually have a larger bond strength (also referred to as bond capacity or bond resistance) at the interface of the FRP laminate and the concrete substrate. Moreover, the durability and long-term performance of the strengthened structure are also improved as the FRPs are protected by the concrete cover (Peng et al., 2019). The bond strength of the NSM strengthening technique, the maximum tensile force which the interface can bear, is of fundamental importance in practical engineering and needs accurate estimation. Basically, the pull-out test (Fig. 1) (sometimes referred to as the push-pull test) is carried out to measure it.

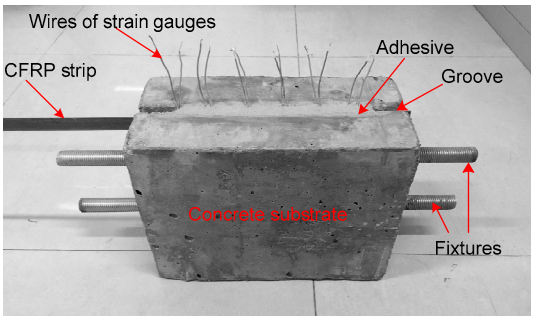

Fig. 1 Pull-out test of near-surface mounted (NSM) carbon fiber-reinforced polymer (CFRP) to concrete joint

Since the bond strength of the NSM strengthening method is different from the EB technology for FRPs, many researchers have conducted extensive experimental (Ceroni, 2010; Zhu et al., 2014; Mahal et al., 2016; Sadoun et al., 2020) and theoretical studies (Petersen et al., 2010; Chen and Cheng, 2016). In these, several reliable bond strength models on the NSM CFRP to concrete joint have been proposed in recent years, and they can be divided into two categories. The first is a statistical model regressed on experimental data. For example, Seracino et al. (2007a) developed a statistical model to predict the maximum debonding force of NSM CFRP joint by using a nonlinear regression analysis on 36 pull-out experimental results. The second is a semi-analytical model based on the fracture-mechanics approach, such as the generic model that can determine the debonding resistance of any adhesive plate-to-concrete joint including the EB and NSM techniques (Seracino et al., 2007b), and the bond strength model based on an existing analytical solution and the fracture energy equation (Zhang et al., 2014), which was considered to be more accurate than the generic model proposed by Seracino et al. (2007b).

However, the raw data for the existing statistical model is limited, and the determination of the critical bond length of the model lacks both theoretical and experimental bases. In addition, the establishment of the semi-empirical model often needs many assumptions, including the forms of the interfacial fracture energy and maximum bond stress, which can be seen from the description in Section 2. Recently, machine learning (ML) methods have been reported to have many successful applications for composite structures. For instance, Vu and Hoang (2016) used the support vector machine (SVM) to estimate the punching shear capacity of FRP reinforced slabs; Karaci et al. (2019) used deep neural network (DNN) and artificial neural network (ANN) to predict material properties of ground-waste-brick mortars. Later, Hoang (2019) employed piecewise multiple linear regression (PMLR) and ANN to predict the properties of steel fiber reinforced slabs. Yang et al. (2019) used the random forest (RF) and the firefly algorithm to predict the dynamic increase factor of steel fiber RC structures. Shishegaran et al. (2020) predicted the maximum deflection of reinforced concrete panels by regression models. Godoy et al. (2020) adopted several ML algorithms to classify quick and highly sensitive clays from measurements. Quite recently, the authors successfully applied ML techniques to identify and predict the properties of FRP composite

structures (Su et al., 2021a, 2021b). By using self-learning, ML is a very powerful artificial intelligence (AI) method. It extracts the complicated relationship between input and output sampling data and then uses that relationship to make predictions or identifications without being explicitly programmed; it provides another method for the evaluation of bond strength.

Among the various ML methods, the ANN is one of the most robust. In this work, we have developed an experimental data-driven back propagation neural network (BPNN) model to predict the bond strength of an NSM CFRP to concrete joint. In addition, the neural interpretation diagram (NID) technique is employed to help interpret the contributions and importance of the input variables in the neural network (NN) due to its black-box nature. NID has been applied in many studies related to the ANN model. For instance, Olden and Jackson (2002b) used it to identify and demonstrate the minor connection weights in the ANN. Abuodeh et al. (2020) combined NID with the ANN to predict the shear strength of FRP strengthening RC beams and to identify the influential input parameters. Hait et al. (2020) adopted NID to visualize the interaction among input variables in the ANN prediction model of damage index of RC buildings.

Inspired by the recent development of ML methods in composite structures, the objective of this paper is to develop an interpretable ANN model with quantized feature importance based on the collected extensive experimental database, to accurately and directly predict the bond strength of the NSM CFRP to concrete joint. The paper contains six sections. Section 2 briefly presents the calculation process of the bond strength of NSM CFRP to concrete joint according to the existing semi-analytical model. This is followed by Section 3 where an extensive experimental database of 163 samples with 10 variables, compiled from the author's research group and from published literature, is collected. In Section 4, the ML methods used in this work are introduced, including the BPNN model and the NID technique. Section 5 outlines the implementation process of the BPNN model employing the NID technique. The preprocessing of the raw data and the searching of the optimal hyperparameters of the ML model are described. Particularly, the relative importance and contributions of the input variables of the proposed BPNN model are quantified by Garson (1991)'s algorithm and the connection weight approach. Then, Section 6 analyzes the prediction performances of the BPNN model and compares the results with the semi-analytical model. A parametric study using the developed BPNN model is also conducted. Lastly, conclusions are summarized.

2 Semi-analytical model of bond strength

In this part, the semi-analytical model, that is the calculation process of the bond strength (P_u) of the NSM CFRP to concrete joint proposed by Zhang et al. (2013, 2014), is given, with the basic equation as follows:

$$P_u=\begin{cases}\sqrt{2G_fE_fA_fC_{failure}}, & L_b\geq L_e,\\ \beta_L\sqrt{2G_fE_fA_fC_{failure}}, & L_b<L_e,\end{cases} \tag{1}$$

where G_f is the interfacial fracture energy, L_b and L_e are the bond length and effective bond length, respectively, E_f and A_f are the elastic modulus and the cross-sectional area of the CFRP strip, respectively, $C_{failure}$ is the dimension of the failure plane in the direction perpendicular to the loading and is taken to be the total length of the three sides of the groove surrounding the concrete, and β_L is a reduction factor to reflect the effect of bond length.

The interfacial fracture energy that is obtained through a regression analysis of numerical results from a finite element model (Zhang, 2012) is determined by

$$G_f=0.4\gamma^{0.422}f_c^{0.619}, \tag{2}$$

where γ is the groove height-to-width ratio, and f_c is the cylinder compressive strength of the concrete. The reduction factor β_L is a function of the bond length, which is determined by

$$\beta_L=\frac{L_b}{L_e}\left(2.08-1.08\frac{L_b}{L_e}\right). \tag{3}$$

The effective bond length can be calculated through

$$L_e = \frac{1.66}{\eta}, \tag{4}$$

$$\eta^2 = \frac{\tau_{max}^2 C_{failure}}{2G_f E_f A_f}, \tag{5}$$

$$\tau_{max} = 1.15\gamma^{0.138} f_c^{0.613}, \tag{6}$$

where η is the coefficient of the governing differential equation for the relationship between the NSM CFRP and concrete, and τ_{max}, which has a similar form with the interfacial fracture energy, is the maximum interfacial shear stress of the NSM CFRP to concrete joint.

3 Data collection

Experimental studies on the bond strength of the NSM CFRP to concrete joint have been conducted, providing an extensive database of pull-out test results of the bonded joints for training and testing the BPNN model. The statistical characteristics of the variables in the database are outlined in Table 1, where t_f is the FRP thickness, mm, h_f is the height of FRP, mm, h_c is the height of concrete block, mm, w_g is the groove width, mm, h_g is the groove height, mm, and a_e is the edge distance, mm.

The details of the raw data are given in Table S1 in the electronic supplementary materials. The database includes 163 testing samples, of which 112 were conducted by the authors' research group in recent years and 51 are collected from the published literature and have been summarized by Zhang (2012). In the database, the material and geometric information of the CFRP strip, the concrete substrate, as well as the groove are considered as the input features, and the bond strength is considered as the target value to be predicted. We randomly divided the whole database into two parts: a training dataset (80%), and a testing dataset (20%).

4 Numerical models

4.1 Back propagation neural network

A main objective of this work is to efficiently fit the relationship between the input features, i.e. the related material and geometric parameters of the pull-out test, and the target variable, that is to say the bond strength of the NSM CFRP to concrete joint. Thus, the ANN model or, more precisely, the BPNN model, is employed to learn the complex patterns in the training data and to make predictions based on new data. The BPNN, regarded as an ensemble of input, output, and hidden layers that transforms the input layer into useful information for the output layer, is a popular ML technique. Each layer of the NN consists of neurons, and each neuron is a mathematical equation expressed as the sum of the weighted inputs:

$$y = a(\boldsymbol{w}\boldsymbol{x} + b), \tag{7}$$

where y is the output, a is the activation function, $\boldsymbol{x}$ is a vector of n inputs, $\boldsymbol{w} \in \mathbb{R}^{1\times n}$ is the weight vector, and b is the bias. In each epoch, the weight vector is updated using the following rule:

$$w := w + \Delta w, \text{ where } \Delta w = -\eta_0 \nabla J(w), \tag{8}$$

where η_0 is the learning rate, and $J(w)$ is the objective function, namely, the cost function (sometimes called the loss function). In order to find the optimal weights of the model, the cost function needs to be globally minimized. Back propagation is a very computationally efficient approach for computing the partial

Table 1 Statistical characteristics of the variables

Item	L_b (mm)	t_f (mm)	h_f (mm)	E_f (MPa)	f_c (MPa)	h_c (mm)	w_g (mm)	h_g (mm)	a_e (mm)	P_u (kN)
Min	30.0	1.2	10.0	129837.0	11.9	150.0	3.0	11.0	20.0	14.8
Max	450.0	20.6	40.0	173000.0	71.1	220.0	35.0	51.0	226.0	205.1
Mean	257.1	3.4	15.7	137925.2	34.2	179.9	11.1	26.7	90.9	65.7
Standard deviation	72.7	2.1	3.4	12711.1	9.4	29.7	5.9	6.9	41.6	27.8

derivatives of the complex cost function in multilayer NNs (Raschka and Mirjalili, 2017). The goal of back propagation is to use these derivatives to determine how changing the weights impacts the overall cost in the NNs and to learn the weight coefficients for parameterizing the NNs (Rumelhart et al., 1986; Nielsen, 2015). The basic steps of back propagation include (1) performing forward propagation and computing the cost error, (2) propagating backward to reduce the error by changing the values of weights and biases, and (3) putting all the weight values together and updating them.

4.2 Neural interpretation diagram

The black box dilemma is the main downside of ANNs, as we are unable to know how specific input variables influence its decision after approximating accurate outputs (Olden and Jackson, 2002b). Therefore, this work combines the NID with the BPNN to analyze the relationship between the input variables and the output based on the experimental dataset of the NSM CFRP to concrete joint. The NID, first presented by Özesmi and Özesmi (1999), aims to provide a visual interpretation of the connection weights among neurons. Researchers can then identify individual and interacting effects of the input features on the output by tracking the magnitude and sign of weights between neurons. Generally, the NID changes the color and thickness of the weight connections in the standard conceptual illustration of the NN to reflect the effect of the input feature, as shown in Fig. 2, where x_1, x_2, x_3 denote input values, $\hat{y}$ denotes the target value, and a_1, a_2, …, a_5 denote activation units. This figure shows a typical single-layer NID where the red line represents a positive weight and the green line represents a negative weight. Moreover, the line thickness is proportional to the absolute magnitude of each weight (Beck, 2018). In Fig. 2, the final effect of each input variable on the output is dependent on the multiplication of the two connection weight directions. For example, positive input-hidden and positive hidden-output connection weights, or negative input-hidden and negative hidden-output connection weights, will result in a positive effect on the output.

However, the interpretation of connection weights is difficult, especially for NNs with many hidden layers and neurons. In this work, we adopt Garson (1991)'s algorithm and a connection weights approach (Olden and Jackson, 2002a) to quantify the relative importance of each individual input variable. Garson (1991)'s algorithm is one of the best-known methods for accessing that importance based on the final weights of the trained NN, and it is still being used. The relative importance of each input feature for a single-layer NN with n input features and m hidden neurons (Ibrahim, 2013; Siu, 2017) is calculated by

$$\mathrm{RI}_i = \sum_{j=1}^{m} \frac{\left|w_{ij} w_{jk}\right|}{\sum_{i=1}^{n} \left|w_{ij} w_{jk}\right|}, \tag{9}$$

where RI_i is the relative importance of the input feature i, $\sum_{i=1}^{n} w_{ij} w_{jk}$ is the sum of the product of the final weights of the connection from an input neuron to hidden neurons with the connection from hidden neurons to an output neuron, j indicates the serial number of hidden neurons, and k indicates the serial number of output neurons. Since Garson (1991)'s algorithm uses the absolute values of the connection weights to calculate the contributions of the input features, it cannot reflect the direction of the weights in the NID.

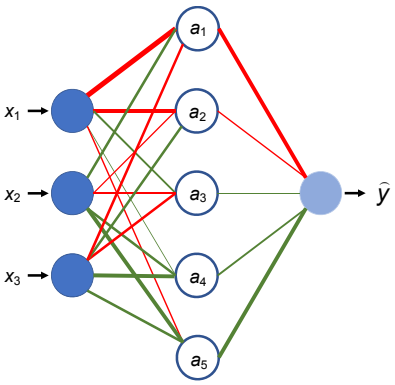

Fig. 2 Example of a neural interpretation diagram (NID)
References to color refer to the online version of this figure

In contrast, the connection weights approach uses the product of the raw input-hidden and hidden-output connection weights and sums the products across all hidden neurons (Olden and Jackson, 2002a). Olden et al. (2004) also indicated that the connection weights approach is better for quantifying feature

importance compared with other commonly used approaches. According to this approach, the relative importance of a given input feature is defined as

$$\mathrm{RI}_i = \sum_{j=1}^{m} w_{ij} w_{jk}. \tag{10}$$

In Section 5.3, we will demonstrate the results of using the two methods to calculate the feature importance of the NID.

5 Implementation of BPNN employing NID

5.1 Data preprocessing

Feature scaling that brings the input variables onto the same scale is a crucial step in the data preprocessing as the BPNN algorithm will behave much better with a noise reduction after this procedure. There are two commonly used techniques to complete the feature scaling procedure: normalization and standardization. Normalization rescales the feature to a range of 0 to 1, such as the min-max scaling. In contrast, standardization centers the feature columns at a mean of zero with a standard deviation of 1 to give them a standard normal distribution; this can be more practical for many ML algorithms such as gradient descent (Raschka and Mirjalili, 2017). The standardization approach is thus used in this study to handle the raw data. For example, $x^{(i)}$ in the input features will have a corresponding new value, $x_{\mathrm{std}}^{(i)}$, calculated by the standardization procedure:

$$x_{\mathrm{std}}^{(i)} = \frac{x^{(i)} - \mu_x}{\sigma_x}, \tag{11}$$

where μ_x is the sample mean of a particular feature column, and σ_x is the corresponding standard deviation.

5.2 Tuning of hyperparameters

The architecture of the BPNN model is defined by the number of hidden layers and neurons, which can be regarded as the hyperparameters that need to be tuned in the ML. Fig. 3 shows the tuning process for selecting the optimum number of neurons to predict the most accurate outputs for the BPNN models with different hidden layers. In order to avoid underfitting or overfitting the training dataset, a 10-fold cross-validation (Jung, 2018) is used to assess the model performance in the tuning process. We randomly split the training dataset into 10 groups, and use nine groups for the model training and the remaining group for validation. Moreover, this procedure is repeated 10 times on the training dataset during each tuning process. It is worth mentioning that the average root mean square error (RMSE) of the 10 folds is adopted as the model score for evaluating the performance of the configuration of the hyperparameters. RMSE is defined as follows:

$$\mathrm{RMSE} = \sqrt{\frac{1}{n}\sum_{i=1}^{n}(y_i - \hat{y}_i)^2}, \tag{12}$$

where n is the number of samples, y_i is the ith predicted value, and $\hat{y}_i$ is the ith ground truth value.

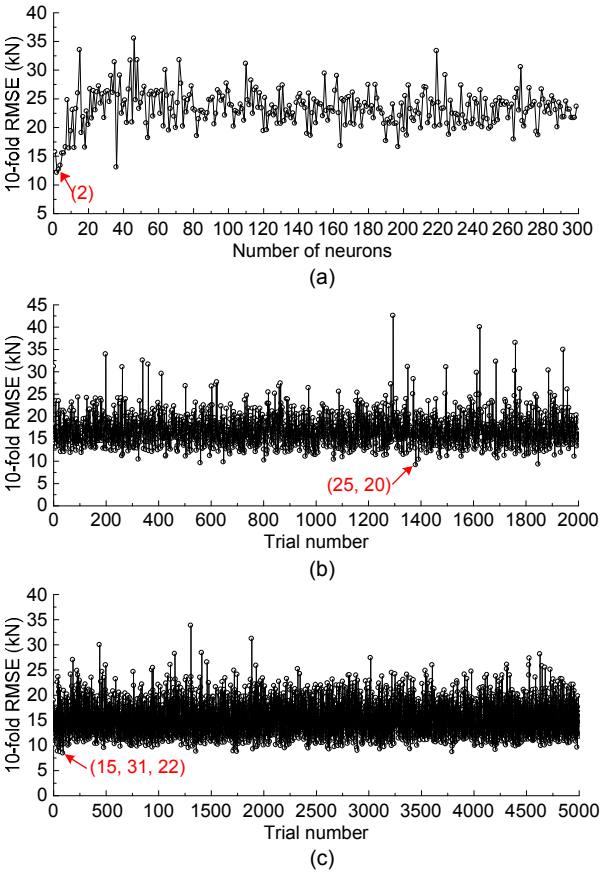

Fig. 3 RMSE during hyperparameter tuning process
(a) BPNN with one hidden layer; (b) BPNN with two hidden layers; (c) BPNN with three hidden layers

Thus, the BPNN models with one hidden layer, two hidden layers, and three hidden layers are tuned and tested (Fig. 3). The BPNN models with four or more hidden layers are not considered as they may cause overfitting problems for a database of the size in this study. For the single-hidden-layer BPNN, the maximum number of neurons is capped at 300. However, it is observed that the average RMSE does not decrease with increase of neurons. On the contrary, the hidden layer with two neurons has the lowest RMSE with a value of 12.14 kN, indicating that the single-hidden-layer BPNN is not suitable for the database in this study.

For the BPNN models with two and three layers, the optimization process becomes extremely computation costly if the grid search technique is adopted. Therefore, a more efficient method, that of the random search, is employed. Random search sets up a grid of hyperparameter combinations and selects random ones to train and score the model instead of doing this for every combination of hyperparameters (Padierna et al., 2017). Its chosen candidates are based on the fly following a random search strategy (Bergstra and Bengio, 2012). Hence, if the random search and the grid search explore exactly the same space of parameters, the run time of a random search to find the optimal hyperparameters is much less. The number of neurons of each hidden layer for the two- or three-layer BPNN models is limited to 100. Then, in the tens of thousands of neuron combinations, we set the trial number in the random search to 2000 for the BPNN model with two layers and 5000 for the model with three hidden layers. These numbers of trials are considered large enough to find the best hyperparameters. It can be found that the BPNN with 25 neurons in the first hidden layer and 20 neurons in the second hidden layer has the lowest RMSE (9.125 kN) for the two-hidden-layer model (Fig. 3b), while the BPNN with 15 neurons in the first hidden layer, 31 neurons in the second hidden layer, and 22 neurons in the third hidden layer has the lowest RMSE (8.433 kN) for the three-hidden-layer model (Fig. 3c).

Thus, by this systematic tuning process of the hyperparameters, a three-hidden-layer BPNN with a neuron architecture of (15, 31, 22) is chosen as the ML model used in this work, as shown in Fig. 4. In this figure, the aforementioned NID is employed in the model to show the contribution of each input feature on the output. As shown in Fig. 4, the red line represents a positive weight, and the green line represents a negative weight. In addition, the thicker the line, the greater the weight. The implementation of the BPNN model is carried out on Scikit-learn and coded by Python language (Pedregosa et al., 2011). For other important hyperparameters, the rectified linear unit (ReLu) activation function is applied in the model that is optimized by using the limited-memory Broyden–Fletcher–Goldfarb–Shanno (LBFGS) method.

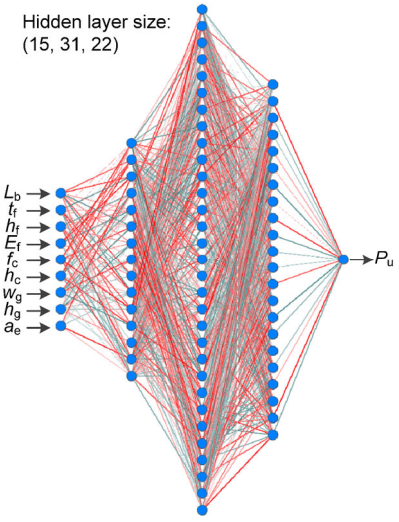

Fig. 4 Architecture of NID-BPNN model with three hidden layers
References to color refer to the online version of this figure

5.3 Feature importance

Garson (1991)'s algorithm and the connection weight approach (described in Section 4.2) are used to interpret the complex relationship of the weights of the NID-BPNN model. It should be noted that the final weights vary slightly with the changes of the initial weights used for the start of the training process of the ANN. To be statistically representative, the BPNN model was executed 10 times and the average results were used as the final weights. Fig. 5 shows the relative importance of input features based on the average final weights of 10 runs of the model. For the experimental database of the NSM CFRP to concrete joint, it is observed that the evaluations of the feature importance are basically consistent whether adopting Garson (1991)'s algorithm or the connection weight approach. Since Garson (1991)'s algorithm uses the absolute

connection weights to calculate variable contributions, it does not give the effect of directions for incoming and outgoing weights in the ANN. However, identifying the feature with negative importance is important because it allows the loss function to rise. That means that the model is not getting good use from the features with negative importance, so removing them can actually improve its performance.

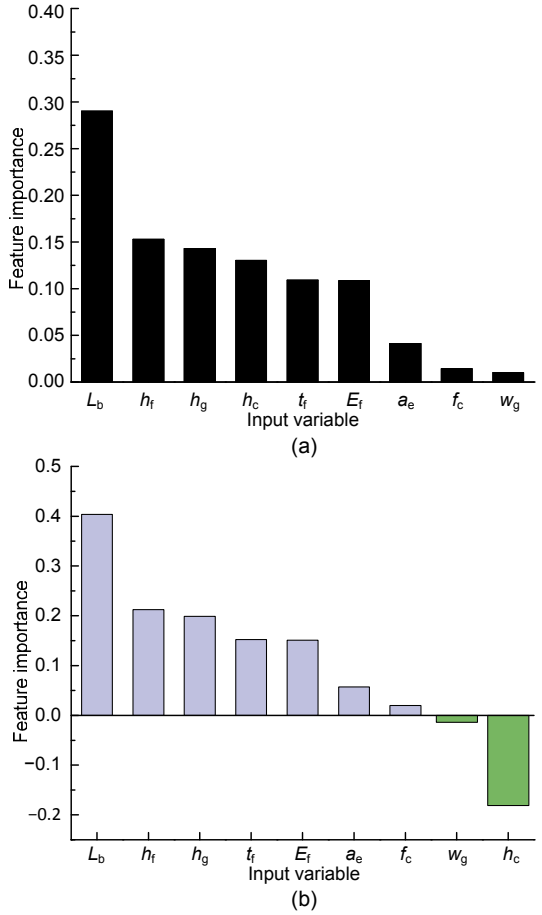

Fig. 5 Feature importance for all input parameters of the experimental database: (a) Garson (1991)'s algorithm; (b) connection weights algorithm

Then, according to the analysis results of the connection weight approach, the groove width (w_g) and the height of concrete (h_c) demonstrate a negative relative importance (Fig. 5b). Otherwise, the rest of the features have a positive relative importance in the model, and the bond length (L_b) has the largest contribution to the NID-BPNN model. These analysis results indicate that the connection weight approach is more accurate than Garson (1991)'s algorithm. Particularly, for the height of concrete, the absolute magnitude of its negative importance is relatively large, but this parameter is considered as an influential feature (rank 4th of the nine input features, Fig. 5a) according to the calculation results of Garson (1991)'s algorithm. In the next section, we will compare the model performance by using the default nine features and the selected features where the feature of the height of concrete is removed.

6 Results and discussion

6.1 Prediction error analysis

In this part, the performance of the proposed BPNN model with default input features and selected features is presented. Again, the model was executed 10 times and the average results were used as the outcomes so as to reliably assess the model prediction error. In addition to the RMSE, the coefficient of determination (R^2), the mean absolute error (MAE), and the mean absolute percentage error (MAPE) are used and defined as follows:

$$R^2 = 1 - \frac{\sum_{i=1}^{n}(y_i - \hat{y}_i)^2}{\sum_{i=1}^{n}(y_i - \bar{y})^2}, \tag{13}$$

$$\mathrm{MAPE} = \frac{1}{n}\sum_{i=1}^{n}\left|\frac{y_i - \hat{y}_i}{\hat{y}_i}\right| \times 100\%, \tag{14}$$

$$\mathrm{MAE} = \frac{1}{n}\sum_{i=1}^{n}\left|y_i - \hat{y}_i\right|, \tag{15}$$

where $\bar{y}$ denotes the mean of the ground truth values.

Fig. 6 shows the predicted output versus actual output of the bond strength for the NSM CFRP to concrete joint, where all the input variables are considered in the model. It is clearly observed that the predictions agree well with the ground truth. Moreover, the R^2 values for the training set, testing set, and all sets are 0.983, 0.900, and 0.957, respectively. Since the R^2 values of the training and testing sets are roughly similar, it is concluded that the BPNN does not overfit the data sample. After removing the input variable of negative feature importance (i.e. the height of the concrete), the prediction performance of the BPNN model using the same configuration of hyperparameters is shown in Fig. 7. There is no obvious change regardless of the prediction errors in the

training process, but the R^2 value slightly increases from 0.900 to 0.915 for the testing set. Therefore, in this case, removing the redundant parameters by incorporating feature importance analysis into the NID-BPNN model can improve its computation efficiency without decreasing its prediction accuracy.

Furthermore, other error indicators including the RMSE, MAE, and MAPE before and after the input feature selection process are calculated, as shown in Table 2. For the testing set, the performances of the BPNN with selected input features (RMSE=10.11 kN, MAE=7.27 kN, MAPE=12.23%) are better than those of the BPNN with default features (RMSE=10.93 kN, MAE=7.47 kN, MAPE=12.86%).

6.2 Comparison with semi-analytical model

The predictions on bond strength of the NSM CFRP to concrete joint produced by the BPNN with

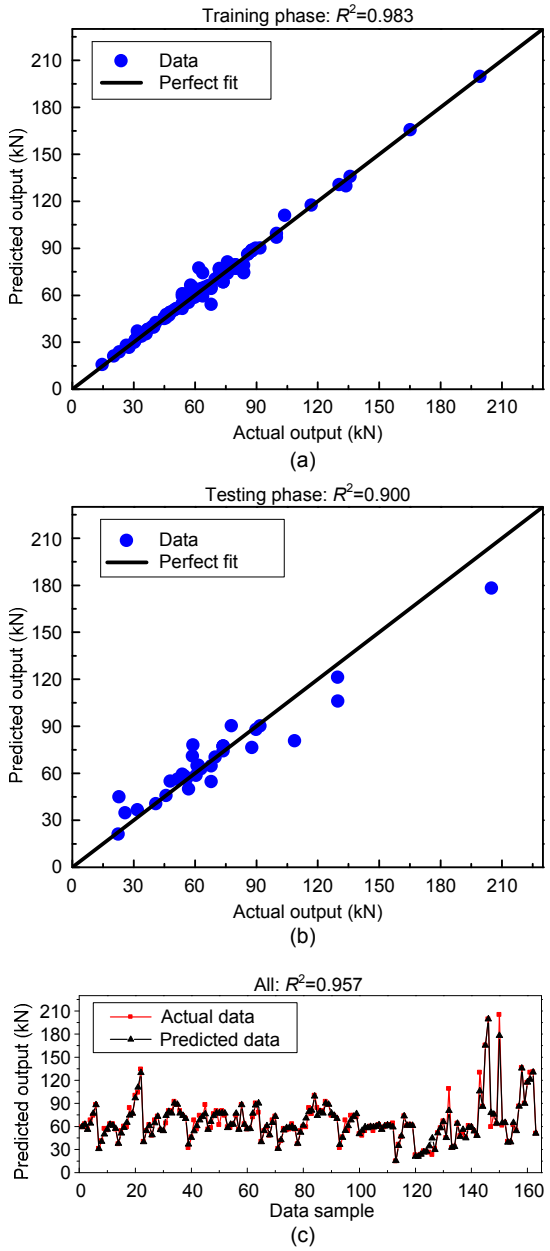

Fig. 6 Prediction results using default input variables: (a) training set; (b) testing set; (c) all sets

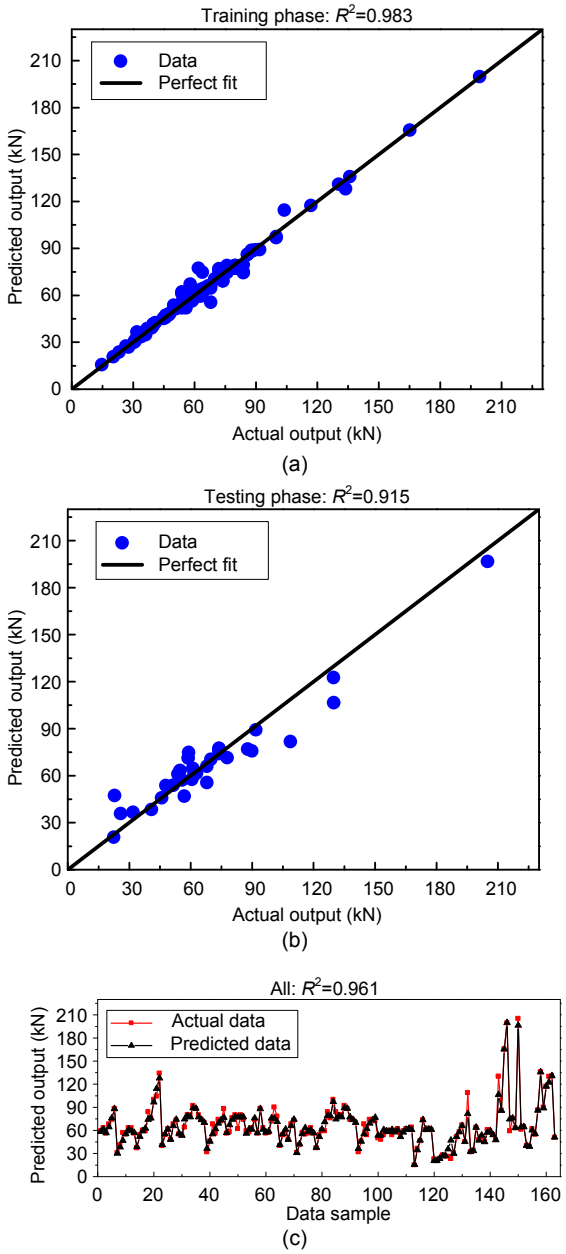

Fig. 7 Prediction results using selected input variables: (a) training set; (b) testing set; (c) all sets

selected input features are compared with those given by the semi-analytical model presented in Section 2. All the samples in the database listed in Table S1 are evaluated by the two methods, and their predictions versus the experimental data plots are shown in Fig. 8. As a result, the semi-analytical model and the BPNN yield R^2 values of 0.761 and 0.961, respectively. In the light of other indicators, the BPNN model also demonstrates a more accurate prediction (RMSE= 5.45 kN, MAE=3.11 kN, MAPE=5.23%) than does the semi-analytical model (RMSE=13.52 kN, MAE= 9.68 kN, MAPE=16.73%), as shown in Table 3. It is worth noting that the proposed ML model need not use any theoretical assumptions but maps the relationship between the input variables and the output based on the experimental database. Therefore, the developed ML method in this study is more direct, simple, and efficient than the existing semi-analytical model.

Table 2 Performance of BPNN with default input variables and selected input variables

BPNN process		Indicator		
		RMSE	MAE	MAPE
Default	Training	3.26	1.85	2.97%
	Testing	10.93	7.47	12.86%
Selected	Training	3.36	2.05	3.29%
	Testing	10.11	7.27	12.23%

6.3 Parametric study

Since the BPNN model cannot directly show the influence of each input variable as the semi-analytical model of bond strength can, a parametric study using the developed BPNN model is described here. Combining the analysis results of the feature importance, a total of six significant parameters are considered, that is, the bond length, the thickness, the height, and the elastic modulus of the CFRP strip, as well as the height and width of the groove. To obtain a reliable result, the values of these parameters are limited within the minimum to maximum ranges of experimental data shown in Table 2.

The bond length has the largest contribution to the prediction of the BPNN according to the research results of Section 5.3. Then, Fig. 9a shows the influence of the variation of the bond length on the bond strength of the NSM CFRP to concrete joint. It can be seen that the bond strength obviously increases with the bond length. Moreover, the larger the cross-sectional area of the CFRP, the larger the bond strength. The effect of the geometric dimensions (i.e. the thickness and the height) and the material properties (i.e. the elastic modulus) of the CFRP on the bond strength are shown in Figs. 9b–9d. Similarly, the three parameters also have a proportional relationship with the bond strength. Besides, when the three parameters are kept constant, the longer the bond

Table 3 Performance of semi-analytical model and BPNN model

Model	Indicator		
	RMSE	MAE	MAPE
Semi-analytical	13.52	9.68	16.73%
BPNN	5.45	3.11	5.23%

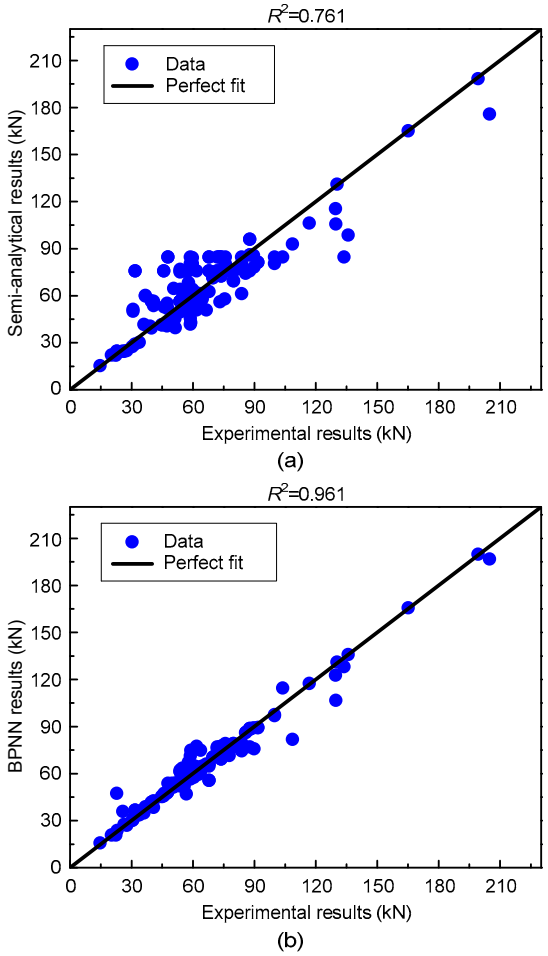

Fig. 8 Prediction results comparison between semi-analytical model (a) and BPNN model (b)

length, the greater the bond strength. As shown in Figs. 9e and 9f, the height of the groove demonstrates a proportional contribution to the bond strength, whereas the bond strength slightly decreases with the increasing width of the groove. Nevertheless, the effect of the variation of the width of the groove is not obvious, which is in consistent with the analysis results of the feature importance where the width of the groove shows a small relative importance among the input features.

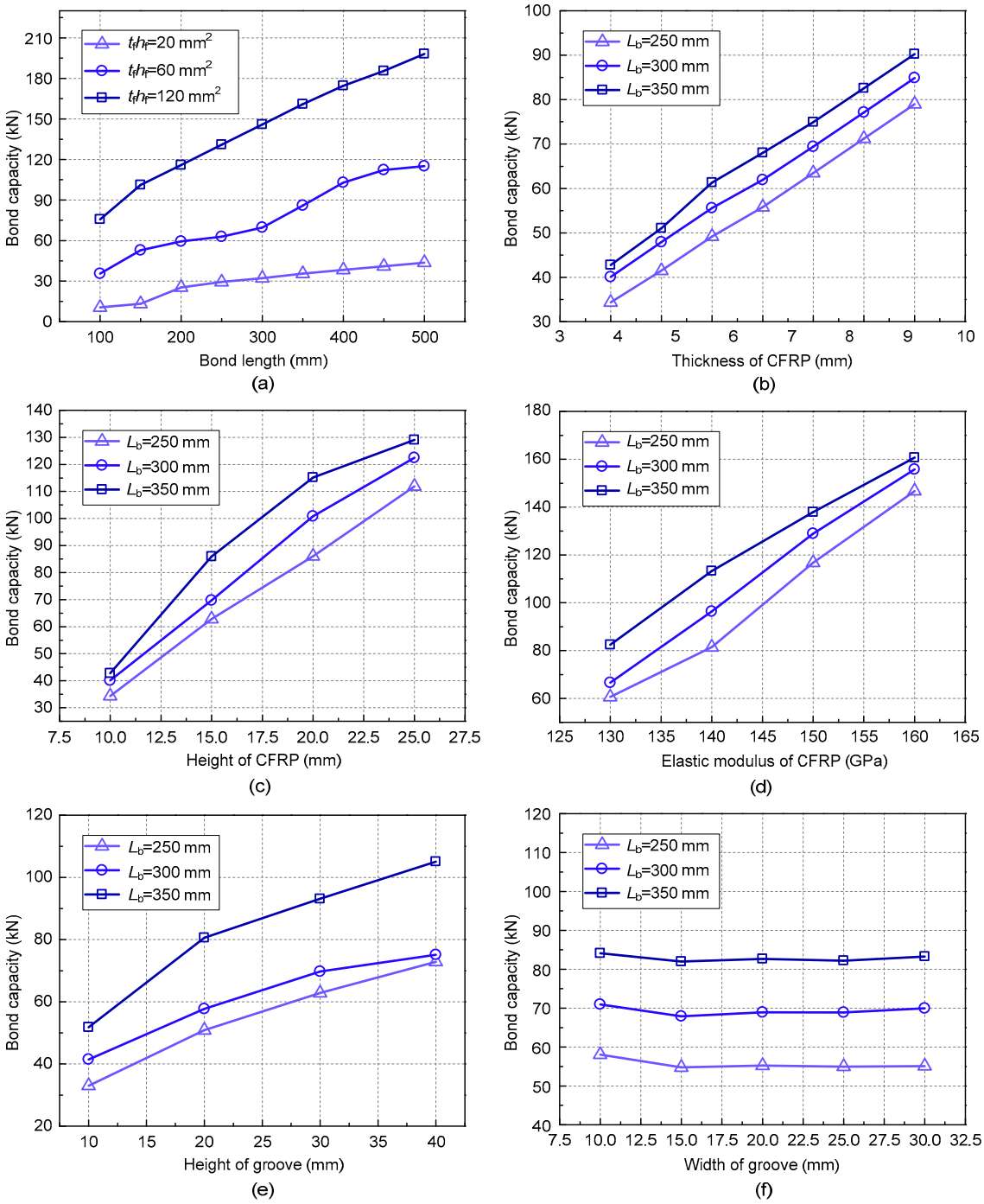

Fig. 9 Parametric study on input variables: (a) bond length; (b) thickness of CFRP; (c) height of CFRP; (d) elastic modulus of CFRP; (e) height of groove; (f) width of groove

7 Conclusions

In this study, we have developed an ANN-based model, i.e. the BPNN model, for predicting the bond strength of an NSM CFRP to concrete joint. An extensive experimental database consisting of 163 test samples is collected from the authors' research group and from the published literature, and is valuable for the research on the NSM CFRP composites. The proposed BPNN model relies on a large experimental database to capture the complex pattern between a set of nine material and geometric input variables and one output value. The prediction error analysis proves that the BPNN can give accurate predictions on the bond strength of the NSM CFRP to concrete joint.

In particular, the NID technique employing Garson (1991)'s algorithm and the connection weight approach is successfully used to quantify the relative importance of the input features, which makes the BPNN model interpretable. The results show that the connection weight approach is more reasonable in determining the feature contribution. After removing one non-significant input feature of the BPNN, the model becomes more computationally efficient, and the R^2 between the predicted values and the ground truth values slightly increases from 0.900 to 0.915. Furthermore, the performance of the BPNN model is compared with the existed semi-analytical model proposed by Zhang et al. (2014) and the developed BPNN approach demonstrates a more accurate prediction (R^2 =0.961, RMSE=5.45 kN) than that of the semi-analytical model (R^2=0.761, RMSE=13.52 kN).

A significant advantage of the proposed ML approach is that it need not use any theoretical assumptions and, therefore, it is more direct, simple, and efficient than the traditional semi-empirical or semi-analytical methods. Moreover, if we keep extending its data samples in the future, it can be expected that the developed BPNN model will become more reliable and powerful.

Contributors

Shao-fan LI designed the research. Hui PENG and Miao SU collected the experiment data. Miao SU wrote the first draft of the manuscript. Shao-fan LI revised and edited the final version.

Conflict of interest

Miao SU, Hui PENG, and Shao-fan LI declare that they have no conflict of interest.

References

Abuodeh OR, Abdalla JA, Hawileh RA, 2020. Prediction of shear strength and behavior of RC beams strengthened with externally bonded FRP sheets using machine learning techniques. *Composite Structures*, 234:111698. https://doi.org/10.1016/j.compstruct.2019.111698

Ali MSM, Oehlers DJ, Griffith MC, et al., 2008. Interfacial stress transfer of near surface-mounted FRP-to-concrete joints. *Engineering Structures*, 30(7):1861-1868. https://doi.org/10.1016/j.engstruct.2007.12.006

Al-Mahaidi R, Kalfat R, 2018. Rehabilitation of Concrete Structures with Fiber-reinforced Polymer. Butterworth-Heinemann, Oxford, UK.

Beck MW, 2018. NeuralNetTools: visualization and analysis tools for neural networks. *Journal of Statistical Software*, 85(11). https://doi.org/10.18637/jss.v085.i11

Bergstra J, Bengio Y, 2012. Random search for hyper-parameter optimization. *Journal of Machine Learning Research*, 13(10):281-305.

Bilotta A, di Ludovico M, Nigro E, 2011. FRP-to-concrete interface debonding: experimental calibration of a capacity model. *Composites Part B: Engineering*, 42(6):1539-1553. https://doi.org/10.1016/j.compositesb.2011.04.016

Ceroni F, 2010. Experimental performances of RC beams strengthened with FRP materials. *Construction and Building Materials*, 24(9):1547-1559. https://doi.org/10.1016/j.conbuildmat.2010.03.008

Chen C, Cheng LJ, 2016. Theoretical solution to fatigue bond stress distribution of NSM FRP reinforcement in concrete. *Composites Part B: Engineering*, 99:453-464. https://doi.org/10.1016/j.compositesb.2016.06.025

Chen YF, Ding DQ, Zhu CH, et al., 2019. Size- and edge-effect cohesive energy and shear strength between graphene, carbon nanotubes and nanofibers: continuum modeling and molecular dynamics simulations. *Composite Structures*, 208:150-167. https://doi.org/10.1016/j.compstruct.2018.10.021

de Lorenzis L, Teng JG, 2007. Near-surface mounted FRP reinforcement: an emerging technique for strengthening structures. *Composites Part B: Engineering*, 38(2):119-143. https://doi.org/10.1016/j.compositesb.2006.08.003

Garson GD, 1991. Interpreting neural-network connection weights. *AI Expert*, 6(4):46-51.

Ghasemi H, Brighenti R, Zhuang XY, et al., 2014. Optimization of fiber distribution in fiber reinforced composite by using NURBS functions. *Computational Materials Science*, 83:463-473. https://doi.org/10.1016/j.commatsci.2013.11.032

Godoy C, I. Depina I, Thakur V, 2020. Application of machine learning to the identification of quick and highly sensitive clays from cone penetration tests. *Journal of Zhejiang University-SCIENCE A (Applied Physics & Engineering)*, 21(6):445-461.

https://doi.org./10.1631/jzus.A1900556

Hait P, Sil A, Choudhury S, 2020. Seismic damage assessment and prediction using artificial neural network of RC building considering irregularities. *Journal of Structural Integrity and Maintenance*, 5(1):51-69. https://doi.org/10.1080/24705314.2019.1692167

Hoang ND, 2019. Estimating punching shear capacity of steel fibre reinforced concrete slabs using sequential piecewise multiple linear regression and artificial neural network. *Measurement*, 137:58-70. https://doi.org/10.1016/j.measurement.2019.01.035

Ibrahim OM, 2013. A comparison of methods for assessing the relative importance of input variables in artificial neural networks. *Journal of Applied Sciences Research*, 9(11): 5692-5700.

Jung Y, 2018. Multiple predicting *K*-fold cross-validation for model selection. *Journal of Nonparametric Statistics*, 30(1):197-215. https://doi.org/10.1080/10485252.2017.1404598

Karaci A, Yaprak H, Ozkaraca O, et al., 2019. Estimating the properties of ground-waste-brick mortars using DNN and ANN. *CMES-Computer Modeling in Engineering & Sciences*, 118(1):207-228. https://doi.org/10.31614/cmes.2019.04216

Mahal M, Täljsten B, Blanksvärd T, 2016. Experimental performance of RC beams strengthened with FRP materials under monotonic and fatigue loads. *Construction and Building Materials*, 122:126-139. https://doi.org/10.1016/j.conbuildmat.2016.06.060

Nielsen MA, 2015. Neural Networks and Deep Learning. Determination Press, New York, USA.

Olden JD, Jackson DA, 2002a. A comparison of statistical approaches for modelling fish species distributions. *Freshwater Biology*, 47(10):1976-1995. https://doi.org/10.1046/j.1365-2427.2002.00945.x

Olden JD, Jackson DA, 2002b. Illuminating the black box: a randomization approach for understanding variable contributions in artificial neural networks. *Ecological Modelling*, 154(1-2):135-150. https://doi.org/10.1016/S0304-3800(02)00064-9

Olden JD, Joy MK, Death RG, 2004. An accurate comparison of methods for quantifying variable importance in artificial neural networks using simulated data. *Ecological Modelling*, 178(3-4):389-397. https://doi.org/10.1016/j.ecolmodel.2004.03.013

Özesmi SL, Özesmi U, 1999. An artificial neural network approach to spatial habitat modelling with interspecific interaction. *Ecological Modelling*, 116(1):15-31. https://doi.org/10.1016/S0304-3800(98)00149-5

Padierna LC, Carpio M, Rojas A, et al., 2017. Hyper-parameter tuning for support vector machines by estimation of distribution algorithms. *In*: Melin P, Castillo O, Kacprzyk J (Eds.), Nature-Inspired Design of Hybrid Intelligent Systems. Springer, Cham, Germany, p.787-800. https://doi.org/10.1007/978-3-319-47054-2_53

Pedregosa F, Varoquaux G, Gramfort A, et al., 2011. Scikit-learn: machine learning in Python. *The Journal of Machine Learning Research*, 12:2825-2830.

Peng H, Liu Y, Cai CS, et al., 2019. Experimental investigation of bond between near-surface-mounted CFRP strips and concrete under freeze-thawing cycling. *Journal of Aerospace Engineering*, 32(1):04018125. https://doi.org/10.1061/(asce)as.1943-5525.0000937

Petersen RB, Masia MJ, Seracino R, 2010. In-plane shear behavior of masonry panels strengthened with NSM CFRP strips. II: finite-element model. *Journal of Composites for Construction*, 14(6):764-774. https://doi.org/10.1061/(asce)cc.1943-5614.0000137

Raschka S, Mirjalili V, 2017. Python Machine Learning: Machine Learning and Deep Learning with Python, Scikit-Learn, and TensorFlow, 2nd Edition. Packt Publishing, Birmingham, UK.

Rumelhart DE, Hinton GE, Williams RJ, 1986. Learning representations by back-propagating errors. *Nature*, 323(6088):533-536. https://doi.org/10.1038/323533a0

Sadoun O, Merdas A, Douadi A, 2020. The bond and flexural strengthening of reinforced concrete elements strengthened with near surface mounted prestressing steel (PS) bars. *Journal of Adhesion Science and Technology*, 34(19): 2120-2143. https://doi.org/10.1080/01694243.2020.1753278

Seracino R, Jones NM, Ali SM, et al., 2007a. Bond strength of near-surface mounted FRP strip-to-concrete joints. *Journal of Composites for Construction*, 11(4):401-409. https://doi.org/10.1061/(asce)1090-0268(2007)11:4(401)

Seracino R, Saifulnaz MRR, Oehlers DJ, 2007b. Generic debonding resistance of EB and NSM plate-to-concrete joints. *Journal of Composites for Construction*, 11(1):62-70. https://doi.org/10.1061/(asce)1090-0268(2007)11:1(62)

Shishegaran A, Khalili MR, Karami B, et al., 2020. Computational predictions for estimating the maximum deflection of reinforced concrete panels subjected to the blast load. *International Journal of Impact Engineering*, 139:103527. https://doi.org/10.1016/j.ijimpeng.2020.103527

Siu C, 2017. Day32: Variable Importance in ANNs. https://csiu.github.io/blog/update/2017/03/28/day32.html

Su M, Peng H, Yuan M, et al., 2021a. Identification of the interfacial cohesive law parameters of FRP strips externally bonded to concrete using machine learning techniques. *Engineering Fracture Mechanics*, 247:107643. https://doi.org/10.1016/j.engfracmech.2021.107643

Su M, Zhong Q, Peng H, et al., 2021b. Selected machine learning approaches for predicting the interfacial bond strength between FRPs and concrete. *Construction and Building Materials*, 270: 121456. https://doi.org/10.1016/j.conbuildmat.2020.121456

Vu DT, Hoang ND, 2016. Punching shear capacity estimation of FRP-reinforced concrete slabs using a hybrid machine learning approach. *Structure and Infrastructure*

Engineering, 12(9):1153-1161. https://doi.org/10.1080/15732479.2015.1086386

Wu YF, Zhou ZQ, Yang QD, et al., 2010. On shear bond strength of FRP-concrete structures. *Engineering Structures*, 32(3):897-905. https://doi.org/10.1016/j.engstruct.2009.12.017

Yang L, Qi CC, Lin XS, et al., 2019. Prediction of dynamic increase factor for steel fibre reinforced concrete using a hybrid artificial intelligence model. *Engineering Structures*, 189:309-318. https://doi.org/10.1016/j.engstruct.2019.03.105

Zhang C, Zhao JH, Rabczuk T, 2018. The interface strength and delamination of fiber-reinforced composites using a continuum modeling approach. *Composites Part B: Engineering*, 137:225-234. https://doi.org/10.1016/j.compositesb.2017.11.007

Zhang SS, 2012. Behaviour and Modelling of RC Beams Strengthened in Flexure with Near-surface Mounted FRP Strips. PhD Thesis, The Hong Kong Polytechnic University, Hong Kong, China.

Zhang SS, Teng JG, Yu T, 2013. Bond-slip model for CFRP strips near-surface mounted to concrete. *Engineering Structures*, 56:945-953. https://doi.org/10.1016/j.engstruct.2013.05.032

Zhang SS, Teng JG, Yu T, 2014. Bond strength model for CFRP strips near-surface mounted to concrete. *Journal of Composites for Construction*, 18(3):A4014003. https://doi.org/10.1061/(asce)cc.1943-5614.0000402

Zhang SS, Yu T, Chen GM, 2017. Reinforced concrete beams strengthened in flexure with near-surface mounted (NSM) CFRP strips: current status and research needs. *Composites Part B: Engineering*, 131:30-42. https://doi.org/10.1016/j.compositesb.2017.07.072

Zhu H, Wu G, Zhang L, et al., 2014. Experimental study on the fire resistance of RC beams strengthened with near-surface-mounted high-T_g BFRP bars. *Composites Part B: Engineering*, 60:680-687. https://doi.org/10.1016/j.compositesb.2014.01.011

List of electronic supplementary materials

Table S1 Experiment database of NSM CFRP to concrete joint